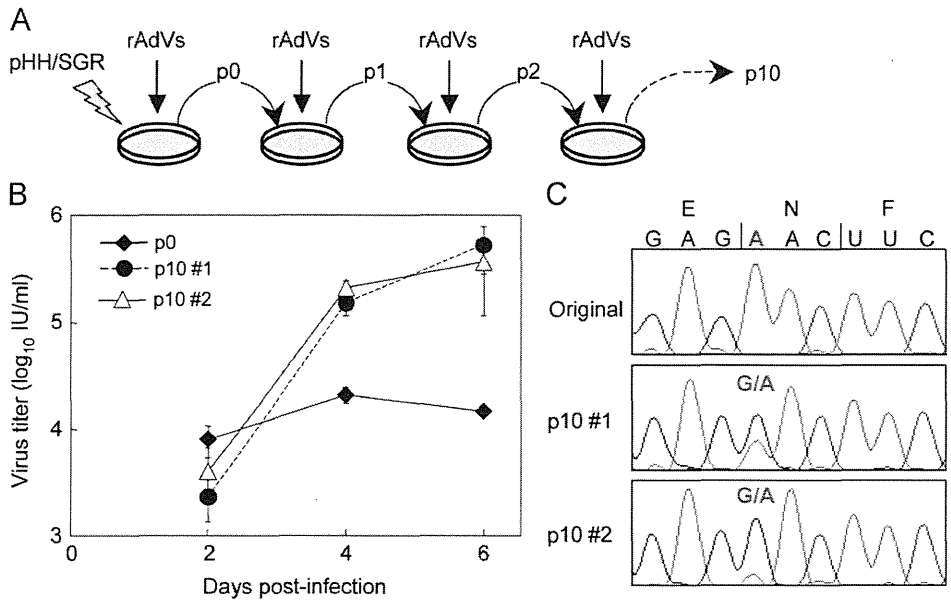

Fig. 6. Genotypic changes in HCVtcp following blind passage. (A) Experimental procedure for blind passage of HCVtcp. Huh7.5.1 cells were transfected with pHH/SGR and were doubly infected with AxCANCre and AxCALNLH-CNS2. Culture fluids were collected and were inoculated into cells infected with AxCANCre and AxCALNLH-CNS2. These procedures were repeated 10 times with two independent samples (#1 and #2). (B) Growth curves of HCVtcp p0 and p10 on Huh7.5.1 cells expressing core-NS2. Cells were infected with HCVtcp at an MOI of 0.05, and medium was collected at the indicated time points and subjected to titration. (C) Nucleotide sequences of original and blind-passaged replicons from HCVtcp. Nucleotides of mutated position are shown in red and bold.

The impact of the N1586D mutation on production of intra- and intergenotypic HCVtcp chimeras was also investigated. The N1586D mutation in the replicon enhanced the production of chimeric HCVtcp by providing core-p7 from all strains examined, although not statistically significant in THpa, and Con1 strains (Fig. 7D). Finally, to determine whether the N1586D mutation was responsible for enhancing HCVcc production, this mutation was introduced into pHHJFH1, which carries the full-length wild-type JFH-1 cDNA (Masaki et al., 2010), yielding pHHJFH1N1586D. The virus titer obtained from cells transfected with the pHHJFH1N1586D was significantly higher than that of WT (Fig. 7E), thus demonstrating that the N1586D mutation enhances yields of HCVcc, in addition to HCVtcp.

Discussion

Single-round infectious viral particles generated by *trans*-packaging systems are considered to be valuable tools for studying virus life cycles, particularly the steps related to entry into target cells, assembly and release of infectious particles. However, limited HCV strains have been applied for the efficient production of HCVtcp to date. In this study, we improved the HCVtcp system in order to enhance the productivity of infectious particles. Production of chimeric HCVtcp by providing genotype 1b-derived core-p7, in addition to intragenotypic viral proteins, was also confirmed. Furthermore, we exploited the system to investigate genetic changes during serial passage of target cells and identified a novel cell culture-adaptive mutation in NS3, which also contributes to enhance the productivity of HCVtcp.

HCVpp (Bartosch et al., 2003a; Hsu et al., 2003) has proven to be a valuable surrogate system by which the study of viral and cellular determinants of the viral entry pathway is possible. Early steps of HCV infection, including the role of HCV glycoprotein heterodimers, receptor binding, internalization and pH-dependent endosomal fusion, have been at least in part mimicked by HCVpp (Lavie et al., 2007). However, as HCVpp is generated in non-hepatic cells such as the human embryo kidney cells 293T, it is likely that the cell-derived component(s) of HCVpp differ from those of HCVcc. Hepatocytes play a role in maintaining lipid homeostasis in the body by assembling and secreting lipoproteins, including VLDL. It is highly likely that HCV exploits lipid synthesis pathways, as there is a tight link between virion formation and VLDL synthesis. Down-regulation of ApoE considerably reduces HCV production (Benga et al., 2010; Chang et al., 2007; Hishiki et al., 2010; Jiang and Luo, 2009; Owen et al., 2009). Infectivity of HCVcc is also neutralized by anti-ApoE antibodies (Chang et al., 2007). These data suggest that ApoE is important for HCV infectivity. Furthermore, Niemann-Pick C1-like 1 (NPC1L1), involving cholesterol uptake receptor, was recently identified as a host factor for HCV entry (Sainz et al., 2012). Knockdown of NPC1L1 had no effect on the entry of HCVpp whereas HCVcc entry was impaired, possibly due to different cholesterol content of these particles. Here, we found that the anti-ApoE antibody neutralized infection by HCVtcp and HCVcc, but not by HCVpp (Fig. 4A and C), thus suggesting that biogenesis and/or secretion pathways of VLDL are involved in HCVtcp similarly to HCVcc, but not in HCVpp.

We also observed that infectivity of HCVtcp and HCVcc is more efficiently neutralized by the anti-CD81 antibody, as compared to that of HCVpp (Fig. 4B and D). It has recently been reported that E2 of HCVcc contained both high-mannose-type and complex-type glycans, whereas most of the glycans on HCVpp-associated E2 were complex-type, which is matured by Golgi enzymes (Vieyres et al., 2010). Mutational analysis of the N-linked glycosylation sites in E1/E2 demonstrated that several glycans on E2 may affect the sensitivity of HCVpp against antibody neutralization, as well as access of CD81 to its binding site on E2 (Helle et al., 2010). The differences in sensitivity between HCVtcp and HCVpp to neutralization by anti-CD81 antibody observed here may be due to differences in carbohydrate composition of HCV glycoproteins during expression and processing of E1/E2 in cells and morphogenesis of HCVtcp and HCVpp.

By analyzing the various replicons for *trans*-packaging, we observed the highest production of HCVtcp with replicons from pHH/SGR, which lacked sequences not essential for RNA

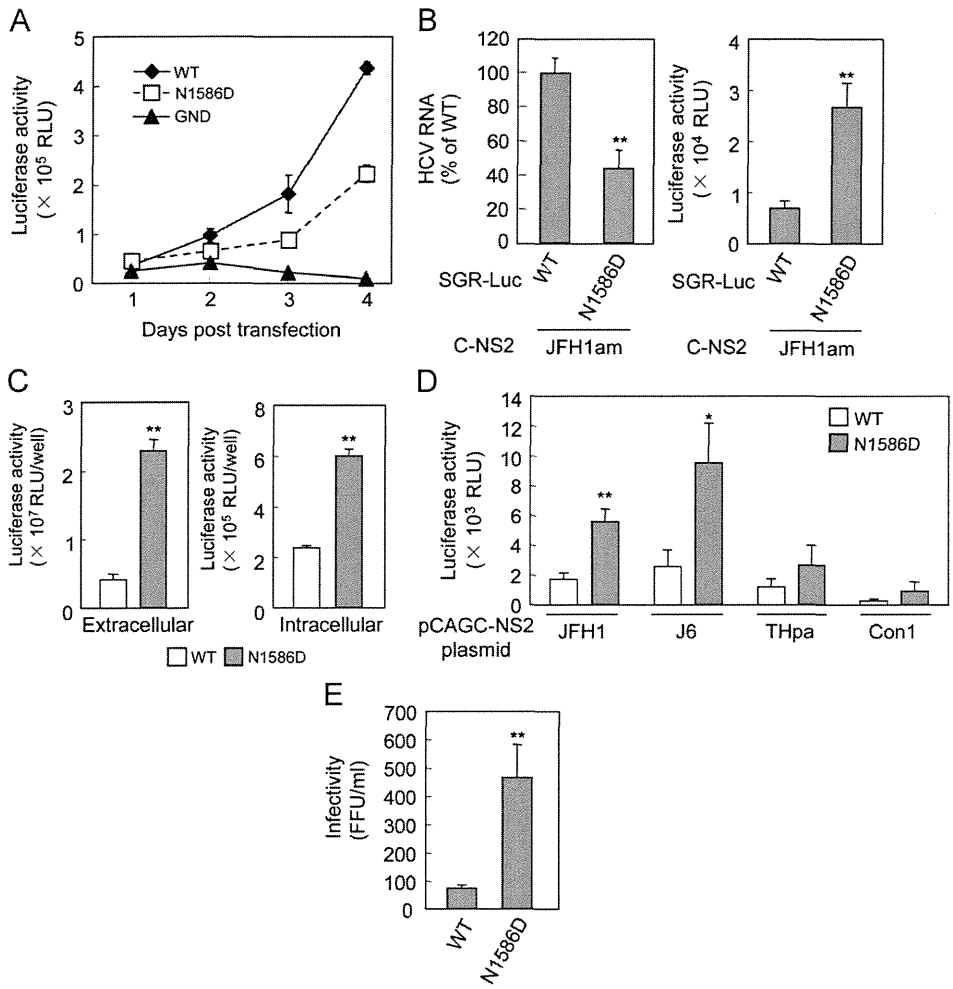

Fig. 7. Effects of N1586D mutation on RNA replication and production of HCVtcp or HCVcc. (A) RNA replication of replicons in cells transfected with pHH/SGR-Luc (WT) or N1586D mutant. Luciferase activities at 1 to 4 day post-transfection were determined. (B) Relative levels of HCV RNA in the supernatants from cells transfected with pHH/SGR-Luc (WT) or N1586D mutant plasmid along with pCAGC-NS2/JFH1am were shown in the left panel. Luciferase activities in cells inoculated with supernatants from cells transfected with indicated plasmids at 4 day post-transfection were shown in the right panel. (C) Luciferase activity in cells inoculated with supernatant and cell lysates from Huh7-25 cells transfected with pHH/SGR-Luc (WT) or N1586D mutant plasmid along with pCAGC-NS2/JFH1am at 5 day post-transfection. (D) Luciferase activity in cells inoculated with culture supernatant from cells transfected with pHH/SGR-Luc (WT) or N1586D mutant plasmid along with indicated core-NS2 plasmids at 4 day post-transfection. (E) Infectivity of supernatant from cells transfected with pHH/JFH1 (WT) or its derivative plasmid containing N1586D mutation at 6 day post-transfection. Statistical differences between WT and N1586D were evaluated using Student's *t*-test. $^{*}p < 0.05$, $^{**}p < 0.005$ vs. WT.

replication, while less efficient productivity was observed from pHH/SGR-Luc, pHH/SGR-C177, pHH/SGR-C191 and pHH/SGR-C-p7/am (Fig. 2C). Differences in the replication efficiency of the replicon do not appear to be a major determinant for HCVtcp productivity, at least in the present settings, as all replicon constructs except pHH/SGR-Luc replicated at similar levels, as confirmed by Western blotting (Fig. 2B). Although the shorter viral genome sequence may offer advantages over the longer sequence, further investigation is required in order to understand the molecular mechanisms underlying viral genome packaging. By comparing pHH/SGR vs. pHH/SGR-C177, pHH/SGR-C191 and pHH/SGR-C-p7/am, it is likely that the expression of the structural protein in *cis* does not increase HCVtcp production when sufficient amounts of structural proteins are supplied in *trans*.

Blind passage of HCVtcp in packaging cells infected with rAdVs providing core-NS2 enabled us to identify a novel culture-adaptive mutation in NS3. The N-terminal third of NS3 forms a serine protease, together with NS4A, and its C-terminal two-thirds exhibits RNA helicase and RNA-stimulated NTPase activities. In addition, similarly to flaviviruses (Kummerer and Rice, 2002; Liu et al., 2002), it is now apparent that HCV NS3 is also involved in viral morphogenesis (Han et al., 2009; Ma et al., 2008), although its precise role and underlying molecular mechanism(s) have not fully been elucidated. Two cell-culture adaptive NS3 mutations which are involved in HCV assembly have been identified. The Q1251L mutation in helicase subdomain 1 resulted in approximately 30-fold higher production of HCV without affecting NS3 enzymatic activities (Ma et al., 2008). The M1290K adaptive mutation was also located in subdomain 1 of the NS3 helicase (Han et al., 2009). The N1586D mutation identified here was located in subdomain 3 of helicase. Analogous to Q1251L and M1290K, the N1586D mutation enhanced the infectious viral assembly by increasing specific infectivity without affecting the efficiency of viral RNA replication. Considering the possibility that NS3 plays a role in linking between the viral replicase and assembly sites (Jones et al., 2011), it is likely that NS3 helicase is one of the determinants for interaction with the structural proteins. Our results, together with earlier studies, suggest that chimeric and defective mutations as well as supplying the viral components in *trans*, function as selective pressures in virion assembly.

In summary, we have established a plasmid-based reverse genetics for efficient production of HCVtcp with structural

proteins from various strains. Single-round infectious HCVtcp can complement the HCVcc and HCVpp systems as a valuable tool for the study of HCV life cycles.

Materials and methods

Cells

Huh7 derivative cell line Huh7.5.1 and Huh7-25 were maintained in Dulbecco modified Eagle medium (DMEM) supplemented with nonessential amino acids, 100 U of penicillin/mL, 100 μg of streptomycin/mL, and 10% fetal bovine serum at 37 °C in a 5% CO_2 incubator.

Plasmids

Plasmids pHHJFH1, pHH/SGR-Luc, pHH/SGR-Luc/GND and pCAG/C-NS2 were as described previously (Masaki et al., 2010). In this study, plasmid pCAG/C-NS2 was designated as pCAGC-NS2/JFH. The plasmid pCAGC-NS2/JFHam having adaptive mutations in E2 (N417S), p7 (N765D), and NS2 (Q1012R) in pCAGC-NS2/JFH was constructed by oligonucleotide-directed mutagenesis. These mutations were also introduced in pHHJFH1, resulting in pHHJFH1am. To generate core-NS2 expression plasmids with different strains of HCV, the cDNA coding core to the first transmembrane region of NS2 (33 amino acids) in pCAGC-NS2/JFH was replaced with the corresponding sequence of the J6 (Lindenbach et al., 2005), H77c (Yanagi et al., 1997), THpa (Shirakura et al., personal communication) and Con1 (Koch and Bartenschlager, 1999) strains. The THpa sequence contained the P to A mutation at 328 aa at E1 in the original TH strain. To generate pHH/SGR, pHH/SGR-Luc was digested with MluI and PmeI, followed by Klenow enzyme treatment and self-ligation to delete the luciferase coding sequence. To generate pHH/SGR-C177, pHH/SGR-C191 and pHH/SGR-C-p7/am, cDNA coding the partial core and luciferase in pHH/SGR-Luc were replaced with coding sequences for mature core (177aa), full-length core (191aa) or core-p7 polyprotein containing adaptive mutations in E2 and p7, respectively. The selected NS3 mutation (N1586D) was introduced into pHH/SGR-Luc and pHHJFH1 by oligonucleotide-directed mutagenesis.

Generation of viruses

HCVcc and HCVtcp were generated as described previously (Masaki et al., 2010). For the production of HCVpp-2a, plasmid pcDNAdeltaC-E1-E2(JFH1)am having adaptive mutations in E2 (N417S) in pcDNAdeltaC-E1-E2(JFH1) (Akazawa et al., 2007) was constructed by oligonucleotide-directed mutagenesis. Murine leukemia virus pseudotypes with VSV G glycoprotein expressing luciferase reporter (VSVpp) were generated in accordance with previously described methods (Akazawa et al., 2007; Bartosch et al., 2003a).

Luciferase assay

Huh7.5.1 cells were seeded onto a 24-well plate at a density of 3×10^4 cells/well 24 h prior to inoculation with reporter viruses. Cells were incubated for 72 h, followed by lysis with 100 μL of lysis buffer. Luciferase activity of the cells was determined using a luciferase assay system (Promega, Madison, WI). All luciferase assays were performed in triplicate.

Quantification of HCV infectivity and HCV RNA

To determine the titers of HCVtcp and HCVcc, Huh7.5.1 cell monolayers prepared in multi-well plates were incubated with dilutions of samples and then replaced with media containing 10% FBS and 0.8% carboxymethyl cellulose. Following incubation for 72 h, monolayers were fixed and immunostained with rabbit polyclonal anti-NS5A antibody, followed by Alexa Fluor 488-conjugated anti-rabbit secondary antibody (Invitrogen), and stained foci or individual cells were counted and used to calculate a titer of focus-forming units (FFU)/mL for spreading infections or infectious units (IU)/mL for non-spreading infections. For intracellular infectivity, the cell pellet was resuspended in culture media, and cells were lysed by four freeze–thaw cycles. Cell debris was pelleted by centrifugation for 5 min at 4000 rpm. Supernatant was collected and used for titration. To determine the amount of HCV RNA in culture supernatants, RNA was extracted from 140 μL of culture medium by QIAamp Viral RNA Mini Kit (QIAGEN, Valencia, CA) and treated with DNase (TURBO DNase; Ambion, Austin, TX) at 37 °C for 1 h. Extracted RNA was further purified by using an RNeasy Mini Kit, which includes RNase-free DNase digestion (QIAGEN). Copy numbers of HCV RNA were determined by real-time quantitative reverse transcription-PCR as described previously (Wakita et al., 2005).

Antibodies

Mouse monoclonal antibodies against actin (AC-15) and CD81 (JS-81) were obtained from Sigma (St. Louis, MO) and BD Biosciences (Franklin Lakes, NJ), respectively. Goat polyclonal antibody to ApoE (LV1479433) was obtained from Millipore (Tokyo, Japan). Anti-NS5A and anti-NS5B antibodies were rabbit polyclonal antibody against synthetic peptides.

Neutralization assay

For neutralization experiments with anti-CD81 antibody, Huh7.5.1 cells were incubated with dilutions of anti-CD81 antibody for 1 h at 37 °C. Cells were then infected with viruses for 5 h at 37 °C. For neutralization experiments with anti-ApoE antibody, viruses were incubated with various concentrations of anti-ApoE antibody at room temperature for 1 h and cells were infected with viruses for 5 h at 37 °C. Following infection, supernatant was removed and cells were incubated with culture medium, and luciferase activity was determined at 3 day post-infection for HCVtcp and pseudotyped viruses. For neutralization experiments with HCVcc generated with pHHJFH1am, a multiplicity of infection (MOI) of 0.05 was used for inoculation, and intracellular core protein levels were monitored by ELISA (Ortho Clinical Diagnostics) at 24 h post-infection.

Immunoblotting

Transfected cells were washed with PBS and incubated with lysis buffer (50 mM Tris–HCl, pH 7.4, 300 mM NaCl, 1% triton X-100). Lysates were then sonicated for 5 min and were added to the same volume of SDS sample buffer. Protein samples were boiled for 10 min, separated by SDS-PAGE, and transferred to PVDF membrane. After blocking, membranes were probed with first antibodies, followed by incubation with peroxidase-conjugated secondary antibody. Antigen–antibody complexes were visualized using an enhanced chemiluminescence detection system (Super Signal West Pico Chemiluminescent Substrate; PIERCE, Rockford, IL), in accordance with the manufacturer's protocols.

Generation of recombinant adenoviruses

rAdV, AxCANCre, expressing Cre recombinase tagged with nuclear localization signal under CAG promoter was prepared as described previously (Baba et al., 2005). The target rAdV AxCALNLH-CNS2 expressing HCV core-NS2 polyprotein with adaptive mutations in E2, p7 and NS2 was generated as follows. Cosmid pAxCALNLwit2 is identical to pAxCALNLw (Sato et al., 1998), except that both the terminal sequences of the rAdV genome are derived from pAxCAwit2 (Fukuda et al., 2006). The core-NS2 fragment obtained from pCAGC-NS2/JFH1am by StuI-EcoRI digestion and subsequent Klenow treatment was inserted into the SwaI site of pAxCALNLwit2. The resultant cosmid pAxCALNLH-CN2it2 was digested with PacI and transfected into 293 cells to generate rAdV AxCALNLH-CNS2.

Preparation of packaging cells for HCVtcp

Huh7.5.1 cells were coinfected with AxCANCre at an MOI of 1 and AxCALNLH-CNS2 at an MOI of 3 for expression of JFH-1 core-NS2 polyprotein containing the adaptive mutations in E2, p7 and NS2.

RNA preparation, RT-PCR and sequencing

Total cellular RNA was extracted with TRIzol reagent (Invitrogen, Carlsbad, CA), and subjected to reverse transcription with random hexamer and Superscript III reverse transcriptase (Invitrogen). Three fragments of HCV cDNAs that cover the entire HCV subgenomic replicon genome, were amplified by nested PCR with TaKaRa Ex Taq polymerase (Takara, Shiga, Japan). Amplified products were separated by agarose gel electrophoresis, and were used for direct DNA sequencing.

Acknowledgments

We are grateful to Francis V. Chisari (The Scripps Research Institute) for providing Huh7.5.1 cells. We thank M. Sasaki, M. Matsuda, and T. Date for their technical assistance, and T. Mizoguchi for the secretarial work. We also thank T. Masaki for their helpful discussions. This work was supported in part by grants-in-aid from the Ministry of Health, Labor, and Welfare and the Ministry of Education, Culture, Sports, Science, and Technology, Japan.

References

Adair, R., Patel, A.H., Corless, L., Griffin, S., Rowlands, D.J., McCormick, C.J., 2009. Expression of hepatitis C virus (HCV) structural proteins in trans facilitates encapsidation and transmission of HCV subgenomic RNA. J. Gen. Virol. 90 (Part 4), 833–842.

Akazawa, D., Date, T., Morikawa, K., Murayama, A., Miyamoto, M., Kaga, M., Barth, H., Baumert, T.F., Dubuisson, J., Wakita, T., 2007. CD81 expression is important for the permissiveness of Huh7 cell clones for heterogeneous hepatitis C virus infection. J. Virol. 81 (10), 5036–5045.

Baba, Y., Nakano, M., Yamada, Y., Saito, I., Kanegae, Y., 2005. Practical range of effective dose for Cre recombinase-expressing recombinant adenovirus without cell toxicity in mammalian cells. Microbiol. Immunol. 49 (6), 559–570.

Bartosch, B., Dubuisson, J., Cosset, F.L., 2003a. Infectious hepatitis C virus pseudoparticles containing functional E1-E2 envelope protein complexes. J. Exp. Med. 197 (5), 633–642.

Bartosch, B., Vitelli, A., Granier, C., Goujon, C., Dubuisson, J., Pascale, S., Scarselli, E., Cortese, R., Nicosia, A., Cosset, F.L., 2003b. Cell entry of hepatitis C virus requires a set of co-receptors that include the CD81 tetraspanin and the SR-B1 scavenger receptor. J. Biol. Chem. 278 (43), 41624–41630.

Benedicto, I., Molina-Jimenez, F., Bartosch, B., Cosset, F.L., Lavillette, D., Prieto, J., Moreno-Otero, R., Valenzuela-Fernandez, A., Aldabe, R., Lopez-Cabrera, M., Majano, P.L., 2009. The tight junction-associated protein occludin is required for a postbinding step in hepatitis C virus entry and infection. J. Virol. 83 (16), 8012–8020.

Benga, W.J., Krieger, S.E., Dimitrova, M., Zeisel, M.B., Parnot, M., Lupberger, J., Hildt, E., Luo, G., McLauchlan, J., Baumert, T.F., Schuster, C., 2010. Apolipoprotein E interacts with hepatitis C virus nonstructural protein 5A and determines assembly of infectious particles. Hepatology 51 (1), 43–53.

Chang, K.S., Jiang, J., Cai, Z., Luo, G., 2007. Human apolipoprotein E is required for infectivity and production of hepatitis C virus in cell culture. J. Virol. 81 (24), 13783–13793.

Cormier, E.G., Tsamis, F., Kajumo, F., Durso, R.J., Gardner, J.P., Dragic, T., 2004. CD81 is an entry coreceptor for hepatitis C virus. Proc. Natl. Acad. Sci. USA 101 (19), 7270–7274.

Evans, M.J., von Hahn, T., Tscherne, D.M., Syder, A.J., Panis, M., Wolk, B., Hatziioannou, T., McKeating, J.A., Bieniasz, P.D., Rice, C.M., 2007. Claudin-1 is a hepatitis C virus co-receptor required for a late step in entry. Nature 446 (7137), 801–805.

Flint, M., von Hahn, T., Zhang, J., Farquhar, M., Jones, C.T., Balfe, P., Rice, C.M., McKeating, J.A., 2006. Diverse CD81 proteins support hepatitis C virus infection. J. Virol. 80 (22), 11331–11342.

Fukuda, H., Terashima, M., Koshikawa, M., Kanegae, Y., Saito, I., 2006. Possible mechanism of adenovirus generation from a cloned viral genome tagged with nucleotides at its ends. Microbiol. Immunol. 50 (8), 643–654.

Han, Q., Xu, C., Wu, C., Zhu, W., Yang, R., Chen, X., 2009. Compensatory mutations in NS3 and NS5A proteins enhance the virus production capability of hepatitis C reporter virus. Virus Res. 145 (1), 63–73.

Helle, F., Vieyres, G., Elkrief, L., Popescu, C.I., Wychowski, C., Descamps, V., Castelain, S., Roingeard, P., Duverlie, G., Dubuisson, J., 2010. Role of N-linked glycans in the functions of hepatitis C virus envelope proteins incorporated into infectious virions. J. Virol. 84 (22), 11905–11915.

Hishiki, T., Shimizu, Y., Tobita, R., Sugiyama, K., Ogawa, K., Funami, K., Ohsaki, Y., Fujimoto, T., Takaku, H., Wakita, T., Baumert, T.F., Miyanari, Y., Shimotohno, K., 2010. Infectivity of hepatitis C virus is influenced by association with apolipoprotein E isoforms. J. Virol. 84 (22), 12048–12057.

Hoofnagle, J.H., 2002. Course and outcome of hepatitis C. Hepatology 36 (5 Suppl. 1), S21–9.

Hsu, M., Zhang, J., Flint, M., Logvinoff, C., Cheng-Mayer, C., Rice, C.M., McKeating, J.A., 2003. Hepatitis C virus glycoproteins mediate pH-dependent cell entry of pseudotyped retroviral particles. Proc. Natl. Acad. Sci. USA 100 (12), 7271–7276.

Ishii, K., Murakami, K., Hmwe, S.S., Zhang, B., Li, J., Shirakura, M., Morikawa, K., Suzuki, R., Miyamura, T., Wakita, T., Suzuki, T., 2008. Trans-encapsidation of hepatitis C virus subgenomic replicon RNA with viral structure proteins. Biochem. Biophys. Res. Commun. 371 (3), 446–450.

Jiang, J., Luo, G., 2009. Apolipoprotein E but not B is required for the formation of infectious hepatitis C virus particles. J. Virol. 83 (24), 12680–12691.

Jones, D.M., Atoom, A.M., Zhang, X., Kottilil, S., Russell, R.S., 2011. A genetic interaction between the core and NS3 proteins of hepatitis C virus is essential for production of infectious virus. J. Virol. 85 (23), 12351–12361.

Kanegae, Y., Lee, G., Sato, Y., Tanaka, M., Nakai, M., Sakaki, T., Sugano, S., Saito, I., 1995. Efficient gene activation in mammalian cells by using recombinant adenovirus expressing site-specific Cre recombinase. Nucl. Acids Res. 23 (19), 3816–3821.

Koch, J.O., Bartenschlager, R., 1999. Modulation of hepatitis C virus NS5A hyperphosphorylation by nonstructural proteins NS3, NS4A, and NS4B. J. Virol. 73 (9), 7138–7146.

Kummerer, B.M., Rice, C.M., 2002. Mutations in the yellow fever virus nonstructural protein NS2A selectively block production of infectious particles. J. Virol. 76 (10), 4773–4784.

Lavie, M., Goffard, A., Dubuisson, J., 2007. Assembly of a functional HCV glycoprotein heterodimer. Curr. Issues Mol. Biol. 9 (2), 71–86.

Lindenbach, B.D., Evans, M.J., Syder, A.J., Wolk, B., Tellinghuisen, T.L., Liu, C.C., Maruyama, T., Hynes, R.O., Burton, D.R., McKeating, J.A., Rice, C.M., 2005. Complete replication of hepatitis C virus in cell culture. Science 309 (5734), 623–626.

Liu, S., Yang, W., Shen, L., Turner, J.R., Coyne, C.B., Wang, T., 2009. Tight junction proteins claudin-1 and occludin control hepatitis C virus entry and are downregulated during infection to prevent superinfection. J. Virol. 83 (4), 2011–2014.

Liu, W.J., Sedlak, P.L., Kondratieva, N., Khromykh, A.A., 2002. Complementation analysis of the flavivirus Kunjin NS3 and NS5 proteins defines the minimal regions essential for formation of a replication complex and shows a requirement of NS3 in cis for virus assembly. J. Virol. 76 (21), 10766–10775.

Ma, Y., Yates, J., Liang, Y., Lemon, S.M., Yi, M., 2008. NS3 helicase domains involved in infectious intracellular hepatitis C virus particle assembly. J. Virol. 82 (15), 7624–7639.

Masaki, T., Suzuki, R., Saeed, M., Mori, K., Matsuda, M., Aizaki, H., Ishii, K., Maki, N., Miyamura, T., Matsuura, Y., Wakita, T., Suzuki, T., 2010. Production of infectious hepatitis C virus by using RNA polymerase I-mediated transcription. J. Virol. 84 (11), 5824–5835.

Mazumdar, B., Banerjee, A., Meyer, K., Ray, R., 2011. Hepatitis C virus E1 envelope glycoprotein interacts with apolipoproteins in facilitating entry into hepatocytes. Hepatology 54 (4), 1149–1156.

McKeating, J.A., Zhang, L.Q., Logvinoff, C., Flint, M., Zhang, J., Yu, J., Butera, D., Ho, D.D., Dustin, L.B., Rice, C.M., Balfe, P., 2004. Diverse hepatitis C virus glycoproteins mediate viral infection in a CD81-dependent manner. J. Virol. 78 (16), 8496–8505.

Owen, D.M., Huang, H., Ye, J., Gale Jr., M., 2009. Apolipoprotein E on hepatitis C virion facilitates infection through interaction with low-density lipoprotein receptor. Virology 394 (1), 99–108.

Pietschmann, T., Kaul, A., Koutsoudakis, G., Shavinskaya, A., Kallis, S., Steinmann, E., Abid, K., Negro, F., Dreux, M., Cosset, F.L., Bartenschlager, R., 2006. Construction and characterization of infectious intragenotypic and intergenotypic hepatitis C virus chimeras. Proc. Natl. Acad. Sci. USA 103 (19), 7408–7413.

Pileri, P., Uematsu, Y., Campagnoli, S., Galli, G., Falugi, F., Petracca, R., Weiner, A.J., Houghton, M., Rosa, D., Grandi, G., Abrignani, S., 1998. Binding of hepatitis C virus to CD81. Science 282 (5390), 938–941.

Ploss, A., Evans, M.J., Gaysinskaya, V.A., Panis, M., You, H., de Jong, Y.P., Rice, C.M., 2009. Human occludin is a hepatitis C virus entry factor required for infection of mouse cells. Nature 457 (7231), 882–886.

Russell, R.S., Meunier, J.C., Takikawa, S., Faulk, K., Engle, R.E., Bukh, J., Purcell, R.H., Emerson, S.U., 2008. Advantages of a single-cycle production assay to study cell culture-adaptive mutations of hepatitis C virus. Proc. Natl. Acad. Sci. USA 105 (11), 4370–4375.

Sainz Jr., B., Barretto, N., Martin, D.N., Hiraga, N., Imamura, M., Hussain, S., Marsh, K.A., Yu, X., Chayama, K., Alrefai, W.A., Uprichard, S.L., 2012. Identification of the Niemann-Pick C1-like 1 cholesterol absorption receptor as a new hepatitis C virus entry factor. Nat. Med. 18 (2), 281–285.

Sato, Y., Tanaka, K., Lee, G., Kanegae, Y., Sakai, Y., Kaneko, S., Nakabayashi, H., Tamaoki, T., Saito, I., 1998. Enhanced and specific gene expression via tissue-specific production of Cre recombinase using adenovirus vector. Biochem. Biophys. Res. Commun. 244 (2), 455–462.

Scarselli, E., Ansuini, H., Cerino, R., Roccasecca, R.M., Acali, S., Filocamo, G., Traboni, C., Nicosia, A., Cortese, R., Vitelli, A., 2002. The human scavenger receptor class B type I is a novel candidate receptor for the hepatitis C virus. EMBO J. 21 (19), 5017–5025.

Steinmann, E., Brohm, C., Kallis, S., Bartenschlager, R., Pietschmann, T., 2008. Efficient trans-encapsidation of hepatitis C virus RNAs into infectious virus-like particles. J. Virol. 82 (14), 7034–7046.

Suzuki, T., Ishii, K., Aizaki, H., Wakita, T., 2007. Hepatitis C viral life cycle. Adv. Drug Deliv. Rev. 59 (12), 1200–1212.

Tani, H., Komoda, Y., Matsuo, E., Suzuki, K., Hamamoto, I., Yamashita, T., Moriishi, K., Fujiyama, K., Kanto, T., Hayashi, N., Owsianka, A., Patel, A.H., Whitt, M.A., Matsuura, Y., 2007. Replication-competent recombinant vesicular stomatitis virus encoding hepatitis C virus envelope proteins. J. Virol. 81 (16), 8601–8612.

Vieyres, G., Thomas, X., Descamps, V., Duverlie, G., Patel, A.H., Dubuisson, J., 2010. Characterization of the envelope glycoproteins associated with infectious hepatitis C virus. J. Virol. 84 (19), 10159–10168.

Wakita, T., Pietschmann, T., Kato, T., Date, T., Miyamoto, M., Zhao, Z., Murthy, K., Habermann, A., Krausslich, H.G., Mizokami, M., Bartenschlager, R., Liang, T.J., 2005. Production of infectious hepatitis C virus in tissue culture from a cloned viral genome. Nat. Med. 11 (7), 791–796.

Yanagi, M., Purcell, R.H., Emerson, S.U., Bukh, J., 1997. Transcripts from a single full-length cDNA clone of hepatitis C virus are infectious when directly transfected into the liver of a chimpanzee. Proc. Natl. Acad. Sci. USA 94 (16), 8738–8743.

Zhong, J., Gastaminza, P., Cheng, G., Kapadia, S., Kato, T., Burton, D.R., Wieland, S.F., Uprichard, S.L., Wakita, T., Chisari, F.V., 2005. Robust hepatitis C virus infection in vitro. Proc. Natl. Acad. Sci. USA 102 (26), 9294–9299.

Biochemical and Biophysical Research Communications 417 (2012) 945–950

Contents lists available at SciVerse ScienceDirect

Biochemical and Biophysical Research Communications

journal homepage: www.elsevier.com/locate/ybbrc

Copy number of adenoviral vector genome transduced into target cells can be measured using quantitative PCR: Application to vector titration

Zheng Pei, Saki Kondo, Yumi Kanegae, Izumu Saito *

Laboratory of Molecular Genetics, Institute of Medical Science, University of Tokyo, 4-6-1 Shirokanedai, Minato-ku, Tokyo 108-8639, Japan

ARTICLE INFO

Article history:
Received 25 November 2011
Available online 19 December 2011

Keywords:
Adenovirus vector
Virus titer
Quantitative PCR

ABSTRACT

Both transfection and adenovirus vectors are commonly used in studies measuring gene expression. However, the real DNA copy number that is actually transduced into target cells cannot be measured using quantitative PCR because attached DNA present on the cell surface is difficult to distinguish from successfully transduced DNA. Here, we used Cre/*lox*P system to show that most of the transfected DNA was in fact attached to the cell surface; in contrast, most of the viral vector DNA used to infect the target cells was present inside the cells after the cells were washed according to the conventional infection protocol. We applied this characteristic to adenoviral vector titration. Current methods of vector titration using the growth of 293 cells are influenced by the effect of the expressed gene product as well as the cell conditions and culture techniques. The titration method proposed here indicates the copy numbers introduced to the target cells using a control vector that is infected in parallel (relative vector titer: rVT). Moreover, the new titration method is simple and reliable and may replace the current titration methods of viral vectors.

1. Introduction

Transfection is the most commonly used method of choice for examining the nature and function of a gene *in vivo* because this technique is very simple to perform and easy to manipulate. However, the copy numbers of DNA that successfully reach the inside of the target cells cannot be measured using quantitative PCR (qPCR), since experiments using qPCR cannot effectively distinguish DNA present inside the cells from DNA attached to and present on the cell surface. The first-generation adenovirus vector (FG AdV) is now commonly used for gene expression experiments, mainly because the resulting expression level is much higher than that achieved using transfection. Another reason is that the data offered by this vector is quantitative for a linearity range that is about 20-fold wider [1]. However, the vector system is also thought to be unsuitable for qPCR for the same reason mentioned above.

There are several methods for using FG AdV. The most popular titration methods are bioassays of plaque-forming unit (PFU) [2,3] and end-point cytopathic effect (CPE) assay or 50% tissue-culture infectious dose ($TCID_{50}$) assay [3,4]. These methods were actually developed for the titration of wild-type adenoviruses, and not for the titration of FG AdV. At least 4 days or up to 2 weeks are required to obtain the endpoint, and the results often vary depending on the conditions of the 293 cell lines, researchers and laboratories. The immunofluorescent focus assay using a florescent microscope [5,6] and the immunospot assay using 3,3′-diaminobenzidine staining [7] (TaKaRa Bio kit), count the foci of infected 293 cells expressing viral hexon protein. Although the titration can be completed in 2 days, these methods also rely on viral replication in 293 cells. The amount of AdV particles has been measured based on the optical density at 260 nm (OD_{260}) [8], although this method can only be used for purified virus stock. Because the AdVs replicate rapidly in growing 293 cells in all these methods, the titration results are sometimes influenced by the expressed product of an inserted gene if it disturbs viral replication or the growth of 293 cells. Consequently, sometimes the results do not reflect the actual copy number that was transferred to the target cells, which is undoubtedly the most important ability of a "vector".

qPCR has been used to calculate the copy numbers of AdV in viral stocks [9]. In the preparation of helper-dependent AdV (HD AdV), the contaminated helper virus (an FG AdV) in the viral stock has been measured using qPCR [10,11]. Another category of the qPCR method obtains the viral titer not by measuring AdV DNA in the viral stock, but by quantifying the copy numbers of *transduced viral genomes in the target cells* (genomic infectious titer,

Abbreviations: FG, first-generation; AdV, adenoviral vector; PFU, plaque-forming unit; $TCID_{50}$, 50% tissue-culture infectious dose; CPE, cytopathic effect; qPCR, quantitative real-time PCR; HD-AdV, helper-dependent AdV; GIT, genomic infectious titer; rVT, relative vector titer; MOI, multiplicity of infection; NLS, nuclear localization signal; OTC, Ornithine transcarbamylase.

* Corresponding author. Fax: +81 3 5449 5432.
E-mail address: isaito@ims.u-tokyo.ac.jp (I. Saito).

0006-291X/$ - see front matter © 2011 Elsevier Inc. All rights reserved.
doi:10.1016/j.bbrc.2011.12.016

GIT); the total DNA of the infected cells were extracted, and the viral DNA were detected using slot-blot hybridization [12] or qPCR [10,13]. Although all these methods are intended to measure the copy number of the viral genome, there are two problems with using them for the titration of FG AdV. One reason is similar to that described above for transfection but is more crucial: the obtained copy numbers include not only the viral genome of the internally transduced viral particles, but also the DNA of *non-infectious particles* and unpackaged naked DNA that is present either freely in the viral stock or attached to the surface of the target cells. The other problem is that the GIT fluctuates markedly depending on the target cell concentration and conditions; hence, GITs obtained at different times and places are difficult to compare. Therefore, both of these problems must be solved to establish a reliable GIT method. In this paper, we propose a new titration method that solves these problems.

2. Materials and methods

2.1. Cell lines and recombinant adenovirus

The human embryo kidney cell line 293 [14] constitutively expresses adenoviral E1 genes. The cell line CV-1 is derived from African green monkey kidney. HeLa cells are derived from human cervical cancer. The cell line NIH-3T3 was established from an NIH Swiss mouse embryo. AxCANCre, a Cre-expressing AdV tagged with a nuclear localization signal [15], and AxEFdsR, a dsRed-expressing AdV [16], have been described previously. The GFP-expressing AdV AxCAGFP was generated using the COS-TPC method [17]. The AdV AxEFLNLdsRed is identical to AxCALNLZ [15] except that the CAG promoter and the LacZ gene were replaced by the EF1α promoter, and the dsRed gene, respectively. The $TCID_{50}$ was measured according to the protocol described by Kanegae et al. [4]. The plasmid pA14cw contains the AdV genomic DNA of pAdex1w [17] from map units 0 to 14.

2.2. Southern blotting analysis

CV-1 cells in a 6-cm dish were infected with AxCANCre. After 24 h, the cells were infected with AxEFLNLdsRed or transfected with 1 μg of the plasmid pxEFLNLdsRed per 6-cm dish using Transfast (Promega). The total DNA was prepared from the dish [18]. Before alkaline treatment, the agarose gel was exposed to 0.1-N HCl for partial depurination causing DNA fragmentation to several hundred base pairs (bp) to obtain the complete transfer to the membrane [19]; the DNA was then transferred to the nylon membrane Hybond-N (Amersham GE) using the capillary-transfer method [20]. Specific DNA was detected using a DIGDNA Labeling and Detection Kit (Roche Diagnostics). The 0.6-kb *Xmn*I fragment derived from the EF1α promoter region was labeled with digoxigenin-UTP, and specific DNA was detected using the chemiluminescence of CDP-Star (Roche Diagnostics). The bands were visualized using LAS-4000 (Fuji Film) and the densitometry was performed using an image analysis program (Multi Gauge version 3X, Fuji Film). The linear correlation between the DNA amounts and the intensity of the bands was confirmed (Fig. S1 of Supplementary Data), showing that the Southern analysis was quantitative.

2.3. qPCR

The infected total cell DNA was prepared from cells, as described previously [18,21]. Alternatively, we confirmed the total cell DNA prepared using a DNA preparation kit (Macherey–Nagel through TaKaRa Bio). qPCR was performed to detect the AdV genome using a probe for the pIX gene [16] (Fig. 2A). The amount of chromosomal DNA was simultaneously measured to correct the Ct values of the viral genome per cell, and the corrected Ct was shown throughout. The probes were derived from the sequence of the human β-actin gene for HeLa, the human OTC gene for CV-1 [16], and the mouse GAPDH gene for NIH-3T3 (Applied Biosystems, catalog number 7000-1). The qPCR reaction was performed according to the manufacturer's protocol: 50 °C for 2 min and 95 °C for 10 min, followed by 40 cycles of 95 °C for 15 s and 60 °C for 1 min (Applied BioSystems).

2.4. Generation of a standard curve using qPCR

The copy numbers of the plasmid pA14cw containing the pIX sequences and the cosmid pAxcwit2 [22] containing the full-genome of the FG AdV [22] were calculated according to Puntel et al. [11]. The plasmid and cosmid were serially diluted (Fig. 2B and C). The equivalency between the molecular weight of the plasmid pA14cw and the number of copies was calculated by considering the pA14cw molecular weight and the equivalency between base pairs (pA14cw [4,247 bp]) and Daltons (Da) ($1bp_{Ad5}$ = 678 Da). $Mass_{pA14cw}$ (Da) = 4,247 bp/molecule × 678 Da/bp = 2.88×10^6 Da/molecule. We obtained the equivalency of mass 2.88×10^6 Da/molecule × 1.66×10^{-18} μg/Da = 4.78×10^{-12} μg/molecule. The copy numbers of the cosmid pAxcwit2 (42, 698 bp) were similarly calculated.

3. Results and discussion

3.1. Quantification of internally transduced viral copies in target cells

To establish a reliable GIT method, determining the ratio of successfully internalized viral DNA to DNA that has physically attached to the cell surface (that is, naked viral DNA or DNA in inactivated viral particles in AdV-infected target cells) is essential. To estimate the amounts of the former and the latter, we utilized the Cre/*lox*P system. CV-1 cells were infected with the AdV AxCANCre expressing Cre at an MOI of 5. Then, 24 h later, the cells were infected with the target AdV AxEFLNLdsRed at an MOI of 7.5 or were transfected with 1 μg of the target plasmid pxEFLNLdsRed as a control. The target unit in the AdV and the plasmid contains the same sequences of the EF1α promoter and the dsRed gene flanked by two *lox*Ps (Fig. 1A). The total cell DNA was extracted after the indicated number of days and digested with *Bgl*II; the DNA of the target unit was detected using a Southern technique (Fig. 1B and C). The 2.8-kb band (S2.8) indicates the substrate originally present before Cre-mediated recombination, i.e., the unprocessed substrate, while the 1.5-kb band (R1.5) shows the presence of the recombined product. We considered that the viral DNA and the transfected DNA that are physically attached to the cell surface cannot be processed by Cre and remain as unprocessed substrate.

When the cells were transfected with the target plasmid, the majority of the target DNA remained unprocessed even after 72 h (Fig. 1C, column 6). A densitometry analysis showed that only 9 ± 2% (n = 7) of the DNA was processed substrate. Also, a preliminary experiment showed that when using 3 μg of plasmid DNA, the percentage was 12% (data not shown). These results suggested that most of the transfected DNA was possibly present on the cell surface and that the DNA copy number after transfection did not reflect that of the internalized DNA molecules. In contrast, most of the target viral DNA was processed using Cre-mediated recombination by 2 or 3 days after infection (Fig. 1B, columns 5 and 6); the recombination efficiency was 92 ± 3% (n = 4). Considering that the recombination efficiency must not be 100%, the result suggested that at least 92% of the target viral DNA was present inside the infected cells. Similar results were obtained when using

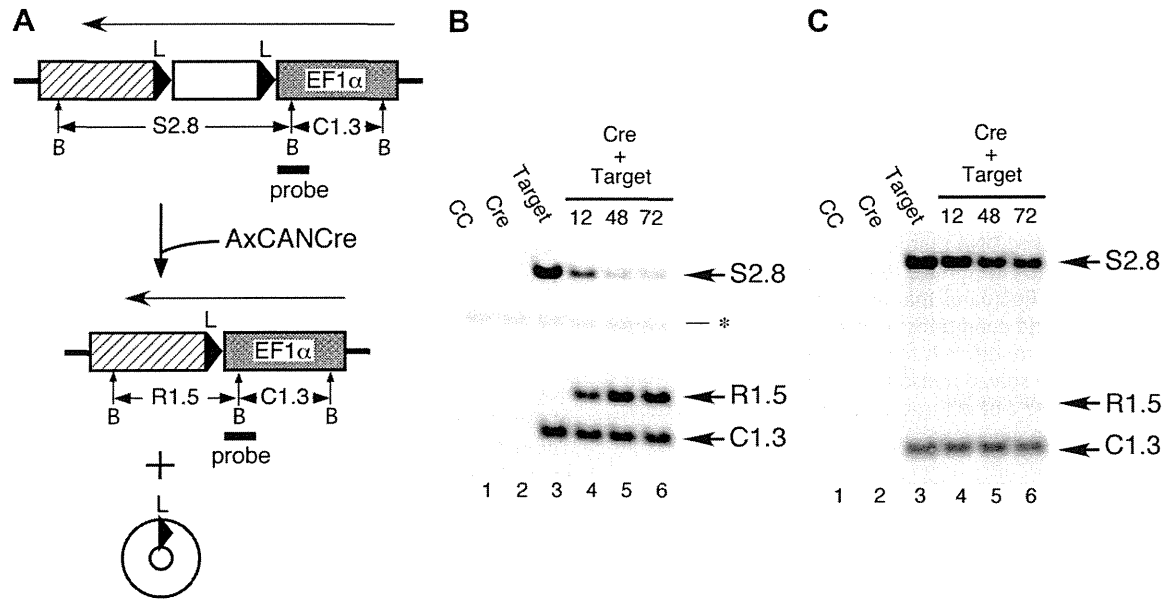

Fig. 1. (A) Structure of the target unit of recipient virus and plasmid. White box, stuffer DNA consisting of neo gene plus polyadenylation (poly(A)) sequence; shadowed box, cDNA plus poly(A) sequence; solid triangle, *lox*P sequence. Arrows show the direction of transcription. (B) Cre-mediated recombination using AdV. CC, uninfected; Cre, AxCANCre; Target, AxEFLNLdsRed. The numbers show the hours after infection. The asterisk shows the sequence of the EF1α gene in the human chromosome. (C) Cre-mediated recombination using plasmid transfection. The representations are the same in (B). For the densitometry four and seven independent experiments in (B) and (C) were performed, respectively.

different MOIs from 1 to 10 (Fig. S2). Therefore, the result showed that nearly all the detected viral DNA was derived from internalized, actively infectious viral particles; hence, the quantification of viral genomes using qPCR can be reliably used for titration.

3.2. Measurement of AdV-genome copies in infected cells using qPCR

A set of TaqMan PCR primers and probes were designed for detecting the AdV genome in the viral pIX coding region, since this gene is present closest to the target insert and encodes a viral structural protein that is essential for stable viral particles (Fig. 2A). The method for quantifying the copy number of FG AdV DNA in infected cells was essentially that described by Ma et al. [9]. The sensitivity of detection and the linear range of the quantification of this qPCR were determined by serial dilution of the 4.2-kb plasmid pA14cw containing the pIX gene and the 42.7-kb cosmid pAxcwit2 containing the full-length genome of the AdV backbone (Fig. 2B and C). The linear range for quantification was found to be between at least 10^3 and 10^9 copies for the plasmid template pA14cw per 5 μL; a plot of the plasmid copy number versus the Ct value between 7 and 27 was linear on a logarithmic scale with a coefficient correlation (r^2) of 0.99 (Fig. 2B). The cosmid template Axcwit2 produced an identical result (Fig. 2C), confirming that the Ct value accurately depended on the copy numbers irrespective of the DNA size. Based on these results, the Ct values obtained using our PCR system can be converted to the copy numbers for a given DNA sample.

As the next step in the titration using qPCR, CV-1 cells in the well of a 24-well plate (2.0×10^5 cells) were infected using the suspension method (see below) with 10 μL of serially diluted stocks of AxCAGFP virus ("control virus stock" for the conversion of the viral Ct value to the copy number *when using our particular qPCR machine*), and the total infected cell DNA was extracted and the Ct values of the viral genome corrected using the Ct value of the cell DNA (see Section 2) were measured (Fig. 2D). A linear correlation of the Ct values to the dilutions was observed from 18 to at least 28. Therefore, together with the results shown in Fig. 2C, the GIT, i.e., the copy number of the transduced viral genome per cell for this cell concentration of 2.0×10^5 cells, can be calculated. For example, a 10^{-2} dilution of 10 μL of viral stock produced a Ct value of 24.34 according to the equation shown in Fig. 2D ($y = 2.97x + 18.4$), and the same Ct value using that shown in Fig. 2C ($y = 24.34 = -3.4x + 38.2$) corresponded to $10^{4.08} \approx 1.2 \times 10^4$ copies of viral genome in 5 μL, i.e., *the GIT titer of the control virus stock was* 2.4×10^8 *copies/mL* ($1.2 \times 10^4 \times 10^3/5 \times 1/10^{-2}$). As described above, because the equations for the plasmid (Fig. 2B) and the cosmid (Fig. 2C) were practically identical, not the cosmid but a plasmid containing the pIX gene can be used for the conversion of the vital Ct value to the copy number. This method of obtaining the GIT of a control virus is essential for rVT because the Ct value differs depending on the qPCR machine. If the $TCID_{50}$ titer of this control virus is known, the $TCID_{50}$ titer can be converted to the copy number/mL (see Section 3.5).

3.3. Establishment of the method for relative vector titer (rVT)

To examine the effect of the cell concentration on the GIT, HeLa cells at densities of 0.6, 2.0 and 6.0×10^5 (full sheet condition) per 6-well plate were infected in parallel with a virus of unknown titer (testing virus) and the virus AxCAGFP (control virus, the same virus used in Fig. 2D). Three days later, the total cell DNA was extracted. For each DNA sample, the Ct values of not only the viral DNA but also the cell chromosome DNA were simultaneously measured to correct for fluctuations in the cell numbers (see Section 2). The transduced copy numbers/mL, i.e. the GIT, vary markedly from 1 to 3.2 and 4.9 in their ratio as reported by Sandig et al. [13] (columns "GIT ratio", lines "HeLa"). This is the second reason why the GIT method cannot be directly used as a titration method. Similar result was obtained when using CV-1 cells (data not shown). In addition to human HeLa cells, monkey CV-1 cells and mouse NIH-3T3 cells were infected with the testing and control viruses and GITs, i.e., the transduced number of copies, were measured (lines "HeLa 6.0", "CV-1 6.0" and "NIH-3T3 6.0"). While the GITs of CV-1 and NIH-3T3 cells were 3-fold and 17-fold lower than that

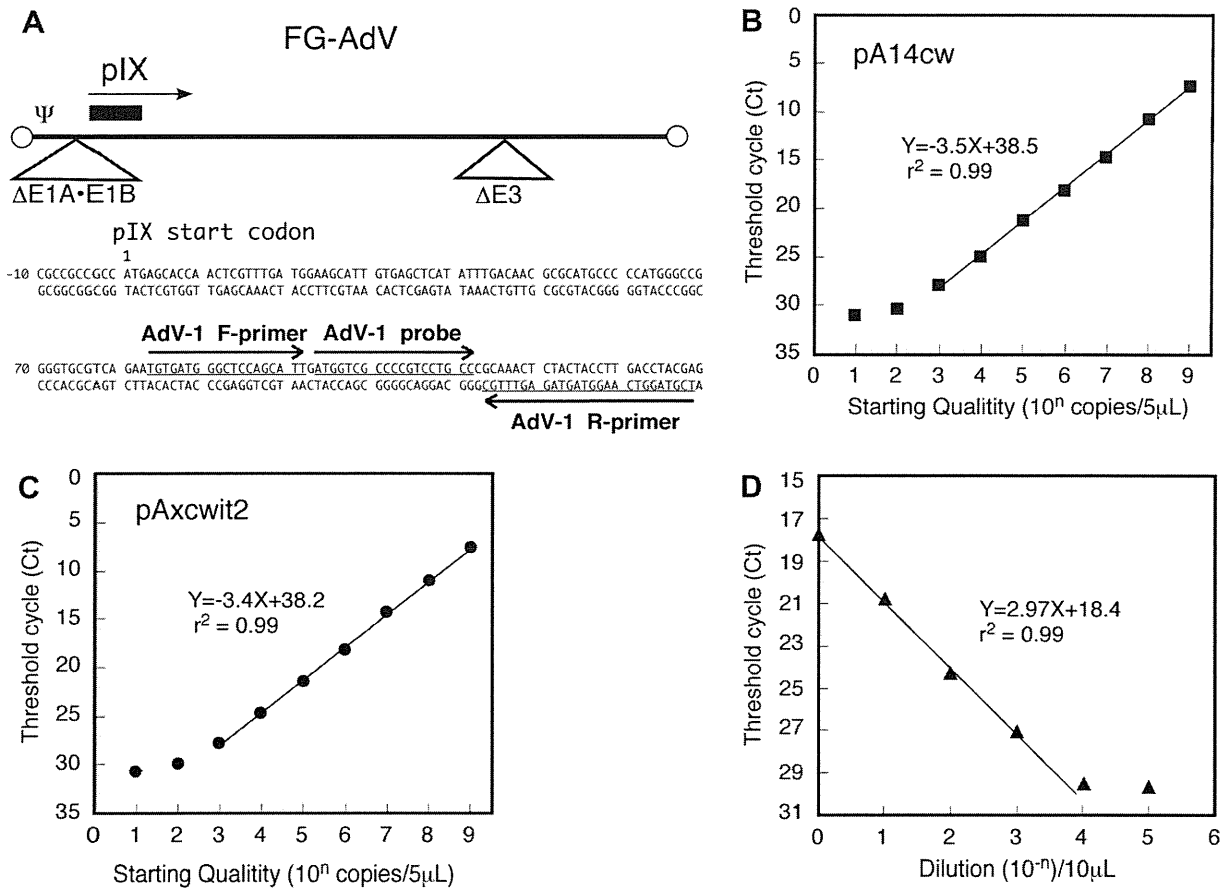

Fig. 2. (A) Position of the AdV-1 primers and the fluorogenic probe. The locations of the packaging signal (Ψ) and the coding region of the pIX gene are indicated. The arrows indicate the direction of transcription. AdV-1 F-primer, R-primer, and probe were designed using the program Primer Express 1.5 (Applied Biosystems), and their sequences are underlined. The primers and probes were selected according to the manufacturer's guidelines. The fluorogenic probes contained FAM (6-carboxylfluoroescein) at the 5′-end and TAMRA (6-carboxyltetramethylrhodamine) at the 3′-end. This set of primers/probe recognizes the coding region of the pIX gene. (B), (C), and (D) are the standard calibration curves for plasmids, cosmids and FG-AdV including the pIX gene, respectively. The standard calibration curves for the threshold cycle values (Ct) versus the copy number using serial dilutions of pA14cw (B) or pAxcwit2 (C) are shown. Similarly, serial dilutions of AxCAGFP vectors were used to generate the standard curve (D). The coefficients of correlation (r^2) are indicated.

of HeLa cells, respectively (column "GIT ratio", 0.3 for CV-1 and 0.06 for NIH-3T3), showing that GIT varied among different cell types.

However, because the control virus infected in parallel was identically influenced by the infection conditions, including the cell concentration and the cell type, the copy numbers of testing virus relative to that of the control virus can be calculated using the Ct value of the control virus as shown below. The relative GIT, called the rVT, is defined as follows:

$$\text{rVT} = (\text{control virus GIT}) \times 2^{(\text{control viral Ct} - \text{testing viral Ct})} (/\text{mL})$$

(Note that, because one *lower* Ct value means 2-fold *more* DNA, "$2^{(\text{testing viral Ct} - \text{control viral Ct})}$" is not correct).

For example, if control virus GIT, control viral Ct and testing viral Ct are 2.4×10^8 (copies/mL), 22.6 and 19.4, respectively, in a particular titration using CV-1 cells, the $\text{rVT} = 2.4 \times 10^8 \times 2^{(22.6-19.4)} = 2.4 \times 10^8 \times 2^{3.2} = 2.2 \times 10^9$ (copies/mL).

Because the rVTs of CV-1 and HeLa cells at the concentrations of 6.0×10^5 cells per well (full-sheet condition) were similar, i.e., 2.3×10^9 (copies/mL), the rVT calculated using the data of Fig. 2D can be applied to the rVT of HeLa cells. The rVTs measured using HeLa cell concentrations of 0.6×10^5, 2.0×10^5 and 6.0×10^5 cells per well were 0.9×10^9, 1.0×10^9 and 2.3×10^9 copies/μL, respectively (Table 1, rVT/mL): the ratio of rVTs obtained using three different cell concentrations (column "rVT ratio") was 0.4:0.4:1. Similar experiments using CV-1 cells indicated that the ratio was 1.2:1.2:1, showing that the rVT was less influenced by the cell concentration than the GIT. Table 1 also showed that, though the GIT of NIH-3T3 was extremely different from that of HeLa and CV-1, the rVT of NIH-3T3 was very similar to those of CV-1 and HeLa (column of "rVT ratio"). Therefore, even using different cell lines and dilutions, the rVT did not fluctuate, indicating that about the same rVT can be obtained using various types of cells other than HeLa cells for the purpose of titration. Because HeLa cells are commonly used worldwide, we recommend the use of HeLa cells for rVT measurements. Importantly, the present results also showed that the

Table 1
Differences between GIT and rVT among various cell concentration and cell lines.

Cells	No. of cells $\times 10^5$	GIT Copies/mL $\times 10^9$	GIT Ratio	rVT rVT/mL $\times 10^9$	rVT Ratio
HeLa	0.6	137.8 ± 6.4	4.9	0.9 ± 0.4	0.4
	2.0	89.5 ± 2.0	3.2	1.0 ± 0.2	0.4
	6.0	28.2 ± 1.8	1	2.3 ± 0.1	1
CV-1	6.0	8.2 ± 1.7	0.3	2.3 ± 0.1	1.0
NIH3T3 6.0	6.0	1.7 ± 0.3	0.06	1.0 ± 0.4	0.4

Two independent experiments were performed using the virus dilutions of 10^1 and 10^2.

Table 2
Infection conditions.

Condition	GIT/mL ($\times 10^9$)	Ratio
Plate	0.8 ± 0.3	1
Suspension	0.8 ± 0.2	1.0

The presentations are the same as Table 1.

Table 3
Days after infections.

Day	GIT/mL ($\times 10^9$)	Ratio
1	2.5 ± 0.1	1.6
2	1.6 ± 0.1	1
3	1.6 ± 0.4	1.0

The presentations are the same as Table 1.

rVT can be compared even when different cell lines or amounts of AdV were used.

The quality of the control virus does not significantly influence on the rVT value as far as the same lot of the control virus is used. Therefore, a conventional virus can be used as the control virus without purification. If strict comparison between the rVTs measured in different laboratories is needed, the adenovirus type 5 reference material may be useful and is available from ATCC (VR-1516) [23]. If a gene product of the testing virus is extremely deleterious to the target cells, the infected cells possibly grow slowly and the ratio of the copy number of the viral genome against that of β-actin on the cell chromosome may increase. However, if this is the case, the obtained rVT values of 10^{-1} dilution (high dose) and 10^{-2} dilution (low dose) must differ significantly, because the latter should be less influenced than the former. We have not experienced these cases.

3.4. Examination of infection conditions

We also examined whether the transduction efficiency of AdV differs when the cells to be infected are attached to a plate (plating method) or present in suspension (suspension method). In the former method, a monolayer of cells on the plate was incubated with an aliquot of AxCAGFP stock for 1 h for 37 °C, with shaking every 15 min before adding the medium. In the latter method, cells detached by trypsin were mixed with the virus, incubated for 5 min at room temperature, mixed with medium, and transferred to a 6-well or 24-well plate. The results showed no significant differences between the two methods for two different virus dilutions (Table 2). Because the suspension method is very simple and quick, we used the suspension method thereafter. Next, we examined the detected copy numbers of the transduced viral genome on days 1, 2 and 3. After washing the cells with PBS (−) on each day, the total infected-cell DNA was extracted, and the amounts of AdV genome were measured using qPCR (Table 3). The detected AdV copy number on day 1 was higher than that on day 2, but those on day 2 and day 3 were equal, suggesting that the number had reached a plateau level. The results were consistent with those for the Southern blot experiments (Fig. 1B, 48 h and 72 h). Consequently, we adopted day 2 for the measurement of rVT. Therefore, for the rVT method the infection protocol is very simple, and titration results can be obtained in only 2 days. The use of the infection protocol is not limited to AdV titration, but can also be used for ordinary AdV infection experiments. The rVT protocol is described in Supplementary Information.

3.5. Examples where the $TCID_{50}$ titer differed from the rVT

The ratio of the rVT value and the authentic $TCID_{50}$ titer were well correlated. AxEFLNLG is one example of an FG AdV; this AdV expresses neo protein unless the neo gene flanked by a pair of *lox*Ps is excised during Cre-mediated recombination. Because the neo gene is popularly used to establish neo-resistant cell lines, it must not be toxic. The rVT/mL and $TCID_{50}$/mL of a viral stock of this AdV were measured using CV-1 cells as a target and 293 cells, in which AdV proliferates, respectively. As shown in Table 4, in the first line, the ratio of rVT/$TCID_{50}$ was 0.3 using CV-1 for rVT; if HeLa cells are used for the rVT, the ratio should be $0.3 \times 0.6 \approx 0.2$ based on the data in Table 1. Thus, the $TCID_{50}$/mL was normally five times higher than the rVT/mL value when using HeLa as the target cells. Therefore, the ratio is normally useful when converting the values from one to another.

Table 4
Differences between rVT and $TCID_{50}$.

AdVs	rVT/mL	$TCID_{50}$/mL	rVT/$TCID_{50}$	Ratio
AxEFLNLG	$0.4 \pm 0.1 \times 10^9$	$1.8 \pm 0.2 \pm 10^9$	0.2	1
AxEFdsRed	$2.3 \pm 0.1 \times 10^9$	$0.3 \pm 0.1 \pm 10^9$	7.7	34.5
AxCANCre	$2.6 \pm 0.4 \times 10^7$	$3.1 \pm 0.9 \pm 10^7$	0.8	3.8

The presentations are the same as Table 1.

However, the ratio sometimes differed; for AxEFdsRed, an AdV that highly expresses dsRed protein, the copy number transduced to the target cells obtained using rVT was 18-times higher than that obtained using the $TCID_{50}$ method. AxCANCre, which highly expresses Cre recombinase, also produced an rVT value that was 3.3-times higher than that obtained using the $TCID_{50}$ method. Because the rVT value reflects the copy numbers in transduced target cells that are important for expression experiments, it is more valuable than the $TCID_{50}$ titer. Also, the rVT method can be applied for the titration of viruses that cannot proliferate in 293 cells, such as HD-AdV and other DNA and RNA viral vectors that do not replicate in the target cells.

In summary, we used Cre recombination and showed that the majority of the AdV genome detected in infected cells indicated successfully transduced molecules and that qPCR can certainly be used for AdV titration. Although cell concentrations and cell types influence the GIT tremendously, these factors can be corrected using a "control AdV" in parallel; hence, we established the rVT method, which can be used to determine the amount of actively infectious AdV genome present in the target cells. This method is quick, reliable, and superior to current titration methods using 293 cells.

Acknowledgments

The authors thank Ms. M. Terashima and Mr. Y. Ohno for technical support. Funding for this research was provided by a Grant in Aid for Scientific Research on Priority Areas from Ministry of Education, Culture, Sports, Science and Technology, Japan (to I.S.).

Appendix A. Supplementary data

Supplementary data associated with this article can be found, in the online version, at doi:10.1016/j.bbrc.2011.12.016.

References

[1] S. Kondo, Y. Takata, M. Nakano, I. Saito, Y. Kanegae, Activities of various FLP recombinases expressed by adenovirus vectors in mammalian cells, J. Mol. Biol. 390 (2009) 221–230.

[2] F.L. Graham, A.J. van der Eb, A new technique for the assay of infectivity of human adenovirus 5 DNA, Virology 52 (1973) 456–467.

[3] B. Precious, W.C. Russell, Growth, purification and titration of adenovirus, in: B.M. Mahy (Ed.), Virology: A Practical Approach, IRL Press, Oxford, 1985, pp. 193–205.
[4] Y. Kanegae, M. Makimura, I. Saito, A simple and efficient method for purification of infectious recombinant adenovirus, Jpn. J. Med. Sci. Biol. 47 (1994) 157–166.
[5] R. Mentel, E. Matthes, M. Janta-Lipinski, U. Wegner, Fluorescent focus reduction assay for the screening of antiadenoviral agents, J. Virol. Methods 59 (1996) 99–104.
[6] L. Philipson, Adenovirus assay by the fluorescent cell-counting procedure, Virology 15 (1961) 263–268.
[7] B. Bewig, W.E. Schmidt, Accelerated titering of adenoviruses, Biotechniques 28 (2000) 870–873.
[8] N. Mittereder, K.L. March, B.C. Trapnell, Evaluation of the concentration and bioactivity of adenovirus vectors for gene therapy, J. Virol. 70 (1996) 7498–7509.
[9] L. Ma, H.A. Bluyssen, M. De Raeymaeker, V. Laurysens, N. van der Beek, H. Pavliska, A.J. van Zonneveld, P. Tomme, H.H. van Es, Rapid determination of adenoviral vector titers by quantitative real-time PCR, J. Virol. Methods 93 (2001) 181–188.
[10] J. Crettaz, C. Olague, A. Vales, I. Aurrekoetxea, P. Berraondo, I. Otano, S. Kochanek, J. Prieto, G. Gonzalez-Aseguinolaza, Characterization of high-capacity adenovirus production by the quantitative real-time polymerase chain reaction: a comparative study of different titration methods, J. Gene Med. 10 (2008) 1092–1101.
[11] M. Puntel, J.F. Curtin, J.M. Zirger, A.K. Muhammad, W. Xiong, C. Liu, J. Hu, K.M. Kroeger, P. Czer, S. Sciascia, S. Mondkar, P.R. Lowenstein, M.G. Castro, Quantification of high-capacity helper-dependent adenoviral vector genomes in vitro and in vivo, using quantitative TaqMan real-time polymerase chain reaction, Hum. Gene Ther. 17 (2006) 531–544.
[12] F. Kreppel, V. Biermann, S. Kochanek, G. Schiedner, A DNA-based method to assay total and infectious particle contents and helper virus contamination in high-capacity adenoviral vector preparations, Hum. Gene Ther. 13 (2002) 1151–1156.
[13] V. Sandig, R. Youil, A.J. Bett, L.L. Franlin, M. Oshima, D. Maione, F. Wang, M.L. Metzker, R. Savino, C.T. Caskey, Optimization of the helper-dependent adenovirus system for production and potency in vivo, Proc. Natl. Acad. Sci. USA 97 (2000) 1002–1007.
[14] F.L. Graham, J. Smiley, W.C. Russell, R. Nairn, Characteristics of a human cell line transformed by DNA from human adenovirus type 5, J. Gen. Virol. 36 (1977) 59–74.
[15] Y. Kanegae, G. Lee, Y. Sato, M. Tanaka, M. Nakai, T. Sakaki, S. Sugano, I. Saito, Efficient gene activation in mammalian cells by using recombinant adenovirus expressing site-specific Cre recombinase, Nucleic Acids Res. 23 (1995) 3816–3821.
[16] Y. Kanegae, M. Terashima, S. Kondo, H. Fukuda, A. Maekawa, Z. Pei, I. Saito, High-level expression by tissue/cancer-specific promoter with strict specificity using a single-adenoviral vector, Nucleic Acids Res. 39 (2010) e7.
[17] S. Miyake, M. Makimura, Y. Kanegae, S. Harada, Y. Sato, K. Takamori, C. Tokuda, I. Saito, Efficient generation of recombinant adenoviruses using adenovirus DNA-terminal protein complex and a cosmid bearing the full-length virus genome, Proc. Natl. Acad. Sci. USA 93 (1996) 1320–1324.
[18] I. Saito, Y. Oya, K. Yamamoto, T. Yuasa, H. Shimojo, Construction of nondefective adenovirus type 5 bearing a 2.8-kilobase hepatitis B virus DNA near the right end of its genome, J. Virol. 54 (1985) 711–719.
[19] I. Saito, R. Groves, E. Giulotto, M. Rolfe, G.R. Stark, Evolution and stability of chromosomal DNA coamplified with the CAD gene, Mol. Cell Biol. 9 (1989) 2445–2452.
[20] J. Sambrook, D.W. Russell, Molecular Cloning, third ed., Cold Spring Harbor Laboratory Press, New York, 2001.
[21] M. Nakano, K. Odaka, Y. Takahashi, M. Ishimura, I. Saito, Y. Kanegae, Production of viral vectors using recombinase-mediated cassette exchange, Nucleic Acids Res. 33 (2005) e76.
[22] H. Fukuda, M. Terashima, M. Koshikawa, Y. Kanegae, I. Saito, Possible mechanism of adenovirus generation from a cloned viral genome tagged with nucleotides at its ends, Microbiol. Immunol. 50 (2006) 643–654.
[23] B. Huchins, N. Sajjadi, S. Seaver, A. Shepherd, S.R. Bauer, S. Simek, K. Carson, E. Aguilar-Cordova, Working toward an adenoviral vector testing standard, Mol. Ther. 2 (2000) 532–534.